Measurement 169 (2021) 108349

Contents lists available at ScienceDirect

Measurement

journal homepage: www.elsevier.com/locate/measurement

Fractal characteristics of acoustic emission of gas-bearing coal subjected to true triaxial loading

Ran Zhang [a,b], Jie Liu [a,b,c,*], Zhanyou Sa [a,b], Zaiquan Wang [d], Shouqing Lu [a,b], Zhaoyang Lv [e,f]

[a] Department of Safety Engineering, Qingdao University of Technology, Qingdao, Shandong 266520, China
[b] Shandong Key Industry Field Accident Prevention Technology Research Center (Non-Ferrous Metallurgy), Qingdao, Shandong 266520, China
[c] Department of Mining Engineering, West Virginia University, Morgantown, WV 26506, USA
[d] School of Science, Qingdao University of Technology, Qingdao, Shandong 266520, China
[e] Institute of Mechanics, Chinese Academy of Sciences, Beijing 100190, China
[f] University of Chinese Academy of Sciences, Beijing 100049, China

ARTICLE INFO

Keywords:
True triaxial
Gas-bearing coal
Acoustic emission
Correlation dimension
Fractal characteristic

ABSTRACT

As coal mining proceeds deeper, coal and rock are subjected to growing stresses and gas pressures. Consequently, coal and rock gas dynamic disasters pose more and more considerable threats and hazards which should be warned in advance. Coal and rock in the field is actually in the true triaxial stress state. Study on deformation characteristics and precursory information of coal and rock under this state is meaningful for disaster warning. In this paper, experiments on the deformation, failure and acoustic emission (AE) characteristics of gas-bearing coal under true triaxial loading conditions were carried out. Besides, the variation law and fractal characteristics of AE under different gas pressures and confining stresses were analyzed. Furthermore, the effects of gas pressure and confining stress on the deformation, failure and fractal characteristics of coal were discussed. The results show that the process of AE variation under true triaxial loading conditions can be divided into two stages, namely the slow growth stage and the accelerated growth stage. A higher gas pressure corresponds to a shorter duration of slow growth stage, while a higher confining stress corresponds to a longer duration of slow growth stage. AE time series has fractal characteristics, and the correlation dimension can characterize the damage degree of a loaded coal sample. The dynamic changes, i.e., fluctuation-increase-decrease, in correlation dimension can accurately reflect the damage evolution process of a coal sample. In addition, the gradual reduction of correlation dimension can be used as the precursor information of coal sample instability and damage. The research results boast instructive significance for preventing the occurrence of coal and rock gas dynamic disasters and for reducing casualties and property loss in coal mines.

1. Introduction

With the increasing demand for energy, shallow coal resources have gradually shrunk, and coal mines have successively entered the stage of deep mining in recent years in China. Continuously deepening coal mining has caused notable changes in stress and gas environment, especially coexistence of high stress and high gas pressure [1–3]. In this complex environment, dynamic disasters in coal mine such as coal and gas outburst (extrusion) and rock burst are occurring more and more frequently and intensely [4–7]. The fact presents high requirements for researches on the mechanism and prevention and control measures of coal mine gas dynamic disasters.

Strain energy accumulated in coal and rock during loading deformation will be dissipated and released during micro-crack propagation. The phenomenon of strain energy release in the form of elastic wave in this process is called acoustic emission (AE) [8–14]. AE, a non-destructive testing method, is widely used for monitoring the deformation and fracturing process of rock materials. Its variation law can reflect the storage and consumption of elastic strain energy within materials. In field mining environment, gas is an essential factor involved in coal mine gas dynamic disasters [15–18]. AE characteristics of gas-bearing coal in the process of loading and fracturing have been extensively researched on. Ma et al. [19] investigated the dynamic adsorption seepage process and AE characteristics of coal, concluding that the AE intensity was the highest in the initial stage of adsorption. Zhao et al. [20] tested the AE characteristics and confining stress effect of gas-

* Corresponding author at: Department of Safety Engineering, Qingdao University of Technology, Qingdao, Shandong 266520, China.
E-mail address: liujie0805@qut.edu.cn (J. Liu).

https://doi.org/10.1016/j.measurement.2020.108349
Received 14 May 2020; Received in revised form 6 August 2020; Accepted 10 August 2020
Available online 15 August 2020

bearing coal under triaxial compression, and analyzed the parameters of AE events. The research by Yin et al. [21] revealed that parameters such as AE, stress and gas flow of gas-bearing coal were well correlated under different stress paths. Niu et al. [22] studied AE characteristics of gas-bearing coal during loading and damage evolution. Kong et al. [23] adopted the critical slowing down theory to explore the variance and auto-correlation coefficient of AE time series of gas-bearing coal under triaxial conditions.

The fractal theory, proposed by Since Mandelbrot [24] in 1977, has been fully applied in various fields. Xie [25] successfully combined fractal geometry with rock mechanics and put forward the concept of fractal rock mechanics. Since then, a large number of studies have been conducted on the fractal characteristics of AE during coal and rock damage. Yin et al. [26] established and analyzed the AE fractal model in the process of rock failure. They believed that the continuous decrease in fractal dimension could be taken as the precursor information of rock instability and failure. Xie et al. [27] probed into the fractal characteristics of AE in the process of layered salt rock failure. Wu et al. [28] found that different rocks exhibited resembling AE fractal characteristics under uniaxial compression. Kong et al. [29] and Li et al. [30] calculated the correlation dimension of AE events of coal under triaxial conditions, holding that the continuous decline in correlation dimension indicated the instability failure of a coal sample. Zhang et al. [31] discussed the AE fractal characteristics of coal samples under uniaxial compression by adopting the single-link cluster method.

Previous studies mainly focused on the test of coal and rock under uniaxial or conventional triaxial conditions. In fact, the occurrence of coal and rock gas dynamic disasters is affected by both three-dimensional stress disturbance and gas. Currently, fractal characteristics of AE of gas-bearing coal subjected to true triaxial loading have been rarely reported. In this paper, a true triaxial loading experiment was performed on coal samples. During the experiments, AE data were acquired for investigating the fractal characteristics of AE time series of coal samples under different gas pressures and different confining stresses. Finally, the effects of gas pressure and confining stress on the fracturing process and fractal characteristics were discussed. The research results boast guiding significance for preventing the occurrence of coal and rock gas dynamic disasters and reducing casualties and property loss in coal mines.

2. Experiment and method

2.1. Sample preparation

In this experiment, raw coal was taken from the working face of No. 2 Coal Mine of Pingdingshan Tian'an Coal Co., Ltd. in Henan Province, China. In hope of maintaining the original state of the coal, a large coal sample was selected and processed into cubical samples with the size of 100 mm × 100 mm × 100 mm. The ends of each sample were smoothed with a millstone to make the roughness smaller than 0.05 mm. As illustrated in Fig. 1(a), the prepared samples were numbered and placed in a constant-temperature incubator for storage. During the experiment, gas injection and deflation is required. In order to ensure the tightness of the entire experimental system, the sample is wrapped with heat shrinkable tube. This will not affect the rupture process of the sample, and the presence of heat shrinkable tube will completely preserve the rupture pattern of the sample, which is conducive to subsequent analysis. When conducting experiments, the samples under different conditions need to be filled with gas at different pressures, so circular hole are reserved on the surface of heat shrinkable tube, as shown in Fig. 1(b).

2.2. Experimental system

The true triaxial gas-bearing coal deformation and failure experimental system consisted of an axial loading subsystem, a confining stress control subsystem, an experiment chamber, a gas seepage subsystem and an AE monitoring subsystem, as shown in Fig. 2. The axial loading subsystem and confining stress control subsystem, together with the experiment chamber, was fixed inside the press. The maximum principal stress σ_1 was controlled by the YAW4306 electro-hydraulic servo pressure testing machine which could achieve displacement loading and stress loading and simultaneously collect and display data in real time. The medium principal stress σ_2 and the minimum principal stress σ_3 were powered by two hydraulic cylinders which could achieve displacement loading and stress loading. The AE monitoring subsystem, i.e., the Express-8 AE equipment (Physical Acoustics Corporation, the United States), was equipped with 8 AE data acquisition channels. The signals acquired by the AE sensors were amplified by the preamplifier and then transmitted to the acquisition card. AE counts, energy, amplitude and other information could be collected in real time through the supporting software AEwin for Express-8.

2.3. Experimental program

Coal is affected by both three-dimensional stress disturbance and gas during working face recovery. A true triaxial loading experiment was designed for simulating the stress and gas conditions in deep mines. In the experiment, the medium principal stress σ_2 was set as 11 MPa, 15 MPa, and 19 MPa, the minimum principal stress σ_3 as 9 MPa, 11 MPa, and 15 MPa, and the gas pressure as 0 MPa, 0.3 MPa, 0.5 MPa, and 0.8 MPa, respectively. The stress path is shown in Fig. 3. Three coal samples were selected under each experimental condition. The experimental

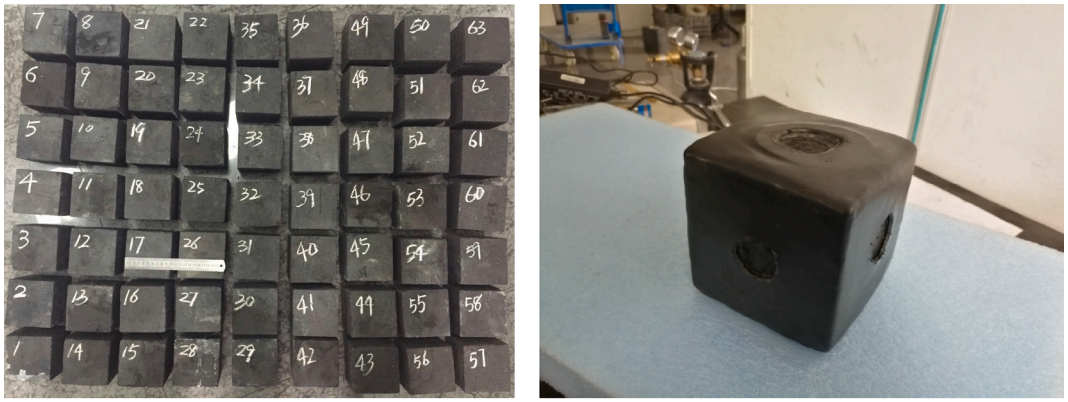

(a) (b)

Fig. 1. Experimental samples.

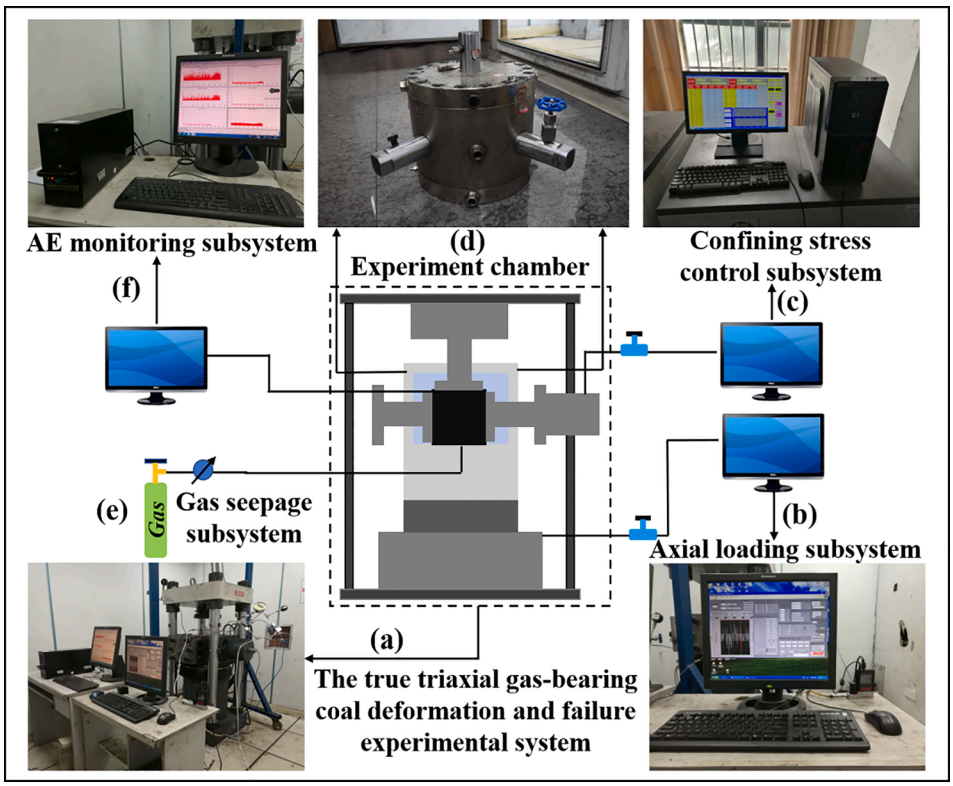

Fig. 2. Schematic diagram of the experimental system (a) The true triaxial gas-bearing coal deformation and failure experimental system; (b) axial loading subsystem; (c) confining stress control subsystem; (d) experiment chamber; (e) gas seepage subsystem; (f) AE monitoring subsystem.

conditions for each coal sample are given in Table 1 (in the table, "TTC" indicates that coal samples are subjected to true triaxial compression, "0" indicates that the gas pressure is 0 MPa, "11" indicates that the medium principal stress σ_2 is 11 MPa, and "1" indicates that the number of coal sample is 1. This nomenclature is applied for other similar terms in the table). The specific experimental procedure is as follows:

(1) The coal sample was placed into the experiment chamber, and then the gas injection and vacuum pumping system was connected to check air tightness.
(2) After the preparation, gas was injected into the chamber according to the experiment conditions. The coal sample was allowed to adsorb gas for 24 h until gas adsorption equilibrium was reached.

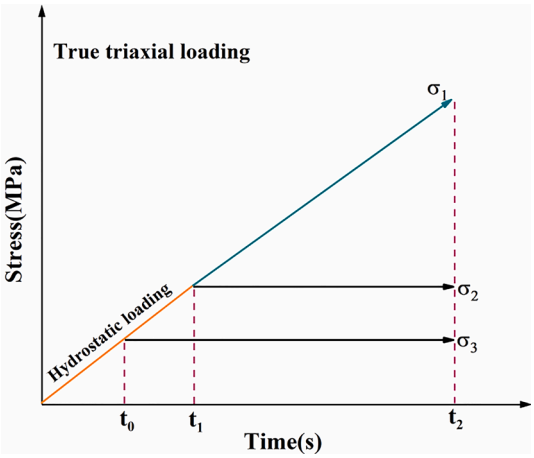

Fig. 3. Stress path diagram.

(3) Stresses σ_1, σ_2 and σ_3 were applied to the coal sample in the mode of hydrostatic loading ($\sigma_1 = \sigma_2 = \sigma_3$) until the set value of σ_3 was reached. Afterwards, with σ_3 maintained constant, the application of stresses σ_1 and σ_2 continued until the set value of σ_2 was reached. Next, with σ_2 kept constant, the axial stress σ_1 was continuously applied at the rate of 500 N/s until the coal sample was destroyed.
(4) Stress, strain and AE data of the sample during in the failure process were simultaneously acquired for subsequent processing.

2.4. Calculation method of fractal characteristic

Grassberger and Procaccia proposed the G-P algorithm in 1983 [32,33]. In light of this algorithm and the phase space reconstruction theory, the correlation dimension of a specific time series, which can reflect the fractal characteristics of the time series, is calculated.

With experimentally obtained AE data taken as the research object, a series of vectors X with a capacity n can be obtained [29]:

$$X = \{x_1, x_2, \ldots, x_n\} \tag{1}$$

where X is the vector in the reconstructed phase space, and n is the capacity of the reconstructed phase space.

The first m numbers in Eq. (1) are regarded as the first m-dimensional phase space vector, as expressed by Eq. (2):

$$X_1 = \{x_1, x_2, \ldots, x_m\} \tag{2}$$

Based on Eq. (2), one more datum is selected backward to obtain a second phase space vector:

$$X_2 = \{x_1, x_2, \ldots, x_{m+1}\} \tag{3}$$

Furthermore, one more datum is selected backward in turn to get $N = n\text{-}m + 1$ vectors, and the correlation function Y is defined as:

Table 1
Experimental conditions of coal samples.

No.	Sample No.	Length (mm)	Width (mm)	Height (mm)	σ_2 (MPa)	σ_3 (MPa)	Gas pressure (MPa)
1	TTC-0-1	100.2	99.6	100.5	19	15	0
2	TTC-0-2	100.2	99.7	101.4	19	15	0
3	TTC-0-3	99.1	100.3	99.6	19	15	0
4	TTC-0.3-1	100.6	99.7	101.2	19	15	0.3
5	TTC-0.3-2	99.2	101.6	100.4	19	15	0.3
6	TTC-0.3-3	100.7	99.5	101.4	19	15	0.3
7	TTC-0.8-1	100.5	101.2	98.6	19	15	0.8
8	TTC-0.8-2	99.6	101.3	99.6	19	15	0.8
9	TTC-0.8-3	99.2	99.5	100.3	19	15	0.8
10	TTC-11-1	100.1	100.5	99.6	11	9	0.5
11	TTC-11-2	98.7	99.5	100.2	11	9	0.5
12	TTC-11-3	99.2	100.3	100.4	11	9	0.5
13	TTC-15-1	99.7	99.3	101.2	15	11	0.5
14	TTC-15-2	101.2	100.1	100.2	15	11	0.5
15	TTC-15-3	98.2	99.5	99.4	15	11	0.5
16	TTC-19-1	100.2	100.6	98.6	19	15	0.5
17	TTC-19-2	99.6	99.1	100.2	19	15	0.5
18	TTC-19-3	100.2	100.1	100.4	19	15	0.5

$$Y(r) = \frac{1}{N^2}\sum_{i=1}^{N}\sum_{j=1}^{N} H\left[r - \left|X_i - X_j\right|\right] \tag{4}$$

where H is the Heaviside function which can be expressed as [30]:

$$H(u) = \begin{cases} 0, u < 0 \\ 1, u \geqslant 0 \end{cases} \tag{5}$$

where r is a given scale function. To avoid dispersion, the value of r can be calculated by:

$$r = k\frac{1}{N^2}\sum_{i=1}^{N}\sum_{j=1}^{N}\left|X_i - X_j\right| \tag{6}$$

where k is the scale factor, and its value takes 0.2, 0.4, 0.6, 0.8, 1.0, 1.2 and 1.4 here because the fractal characteristics of the corresponding time series will become unobvious when $k \leq 0.1$ [34].

There is a correlation function $Y(r)$ corresponding to each given r. The points (lnr, $lnY(r)$) are expressed and fitted in double logarithmic coordinates. If the fitted result is a straight line, the corresponding time series has fractal characteristics at a given scale. In this case, the correlation dimension D is the slope of the fitted straight line:

$$D = lnY(r)/lnr \tag{7}$$

3. Experimental results

3.1. AE time series characteristics

Select the No. 1 sample under each experimental condition for analysis. The experimental results of stress-AE under different gas pressures are presented in Fig. 4. The results show that peak stress of the sample decreases continuously with the increase of gas pressure. The peak stresses under the gas pressures of 0.3 MPa and 0.8 MPa are 15% and 30% lower than the value under 0 MPa respectively, indicating that the presence of gas weakens the bearing capacity and strength of the sample. AE can reflect the damage and destruction process of a sample. As can be seen from Fig. 4, AE exhibits similar variation laws under different gas pressures. As the stress increases, AE count and AE energy both show a rising trend, which corresponds well to damage evolution process of the sample. Meanwhile, the AE variation process under different gas pressures can be divided into two stages, according to accumulative AE count and accumulative AE energy:

(I) Slow growth stage: In this stage, AE signals which mostly belong to paroxysmal signals tend to be gentle, with few AE events occurring. AE count and AE energy remain at low levels, and accumulative AE count and accumulative AE energy grow slowly. The reason is as follows: Under a relatively low stress level, the sample remains basically in the compaction and elastic deformation stage where elastic energy accumulates inside the sample and micro-cracks primarily develop slowly in a small range. Meanwhile, as the gas pressure rises, the duration of slow growth stage shortens: The stage lasts 696 s, 627 s and 415 s under the gas pressures of 0 MPa, 0.3 MPa and 0.8 MPa, respectively. The durations under the gas pressures of 0.3 MPa and 0.8 MPa are 9.9% and 40.3% shorter than that under 0 MPa, respectively, because gas weakens the bearing capacity of a sample and reduces the energy storage threshold of the sample. Moreover, compared with the gas pressure of 0 MPa and 0.3 MPa, the first stage of AE count and energy is relatively high when the gas pressure is 0.8 MPa. This is because under higher gas pressure, gas weakens the bearing capacity of a sample more severely, the pore cracks inside the sample develop faster, releasing more elastic energy, so relatively active AE signal will be generated when the stress level is low.

(II) Accelerated growth stage: When stress exceeds a certain value, AE signal increases significantly; AE count and AE energy grow rapidly; and the corresponding accumulative AE count and accumulative AE energy show a trend of accelerated growth. Under different gas pressures, the stresses corresponding to the significant increase in AE signal differ. As can be observed from Fig. 4, the gas pressures 0 MPa, 0.3 MPa, and 0.8 MPa correspond to the stresses 54.3 MPa, 48.7 MPa, and 32.4 MPa, respectively. That is, the stress falls with the rise of gas pressure. In addition, in the accelerated growth stage, AE displays varying variation laws under different gas pressures. Specifically, when the gas pressure is 0 MPa and 0.3 MPa, large and small AE signals appear alternately, and the occurrence of large signals is paroxysmal. This phenomenon suggests that the damage and failure of the sample is not a continuous process, but a process of micro-crack development, extension and penetration and gradual macro-fracture formation. When the gas pressure is 0.8 MPa, the occurrence of large signals is no longer paroxysmal, which indicates that the sample is the most severely damaged under the gas pressure of 0.8 MPa in comparison with the case under 0 MPa and 0.3 MPa. The result further verifies the effect of gas in weakening the bearing capacity of a coal sample.

The experimental results of stress-AE under different confining stresses are disclosed in Fig. 5. According to the results, the peak stress of the sample increases continuously with the increase in confining stress. The peak stresses under the confining stresses of 15 MPa and 19 MPa are 8.7% and 12.8% higher than the value under 11 MPa, respectively, which demonstrates that the confining stress promotes the strength, energy storage threshold, and bearing capacity of the sample. From Fig. 5, the AE variation laws under different confining stresses resemble those under different gas pressures: AE count and AE energy both rise

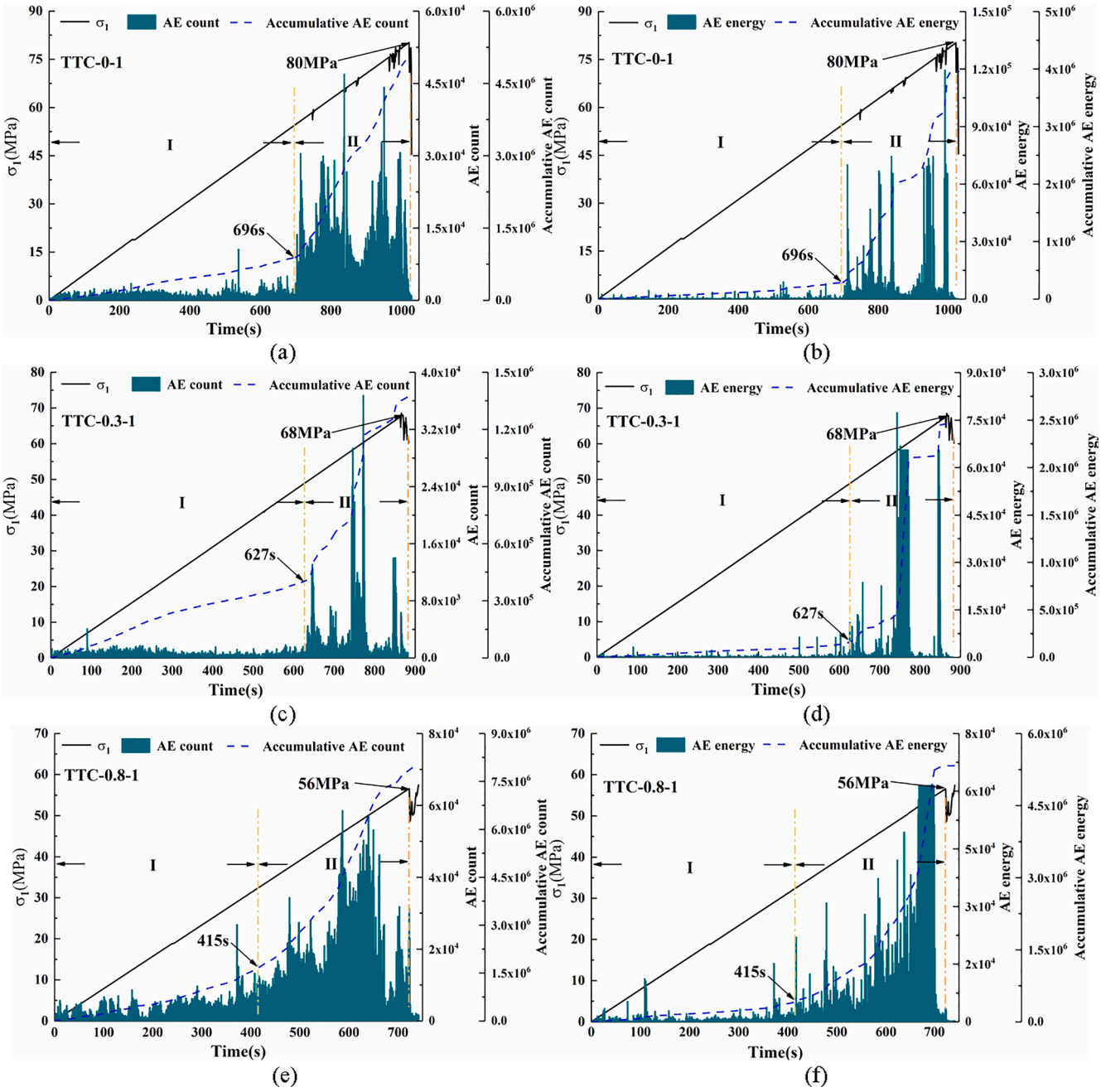

Fig. 4. Experimental results of AE under different gas pressures (a) AE count under 0 MPa; (b) AE energy under 0 MPa; (c) AE count under 0.3 MPa; (d) AE energy under 0.3 MPa; (e) AE count under 0.8 MPa; (f) AE energy under 0.8 MPa.

continuously with the increase in stress, reaching the maximum when the sample nearly completely fails. The two parameters can accurately reflect the damage evolution process of the sample. Meanwhile, the AE variation process under different confining stresses can also be divided into the slow growth stage and the accelerated growth stage, according to accumulative AE count and accumulative AE energy:

(I) Slow growth stage: In this stage, the sample is basically in the hydrostatic loading stage and the early stage of axial continuous loading. Under a low stress level, internal micro-cracks develop poorly and merely expand and extend in a small range. The corresponding AE signals mostly belong to paroxysmal signals whose accumulative AE count and accumulative AE energy grow slowly. Meanwhile, the duration of slow growth stage lengthens as the confining stress rises. The stage lasts 365 s, 455 s and 470 s under the confining stresses of 11 MPa, 15 MPa and 19 MPa, respectively. The durations under confining stresses of 15 MPa and 19 MPa are 24.7% and 28.8% longer than the duration under 11 MPa, respectively, because confining stress promotes the strength and elastic energy storage threshold of the sample.

(II) Accelerated growth stage: When micro-cracks become connected locally, AE signal increases remarkably, and accumulative AE count and accumulative AE energy become more and more active, indicating the entrance of AE into the accelerated growth stage. Under different confining stresses, the stresses corresponding to the entrance differ. As illustrated in Fig. 5, the confining stresses 11 MPa, 15 MPa, and 19 MPa correspond to the stresses 28.8 MPa, 35.7 MPa, and 36.9 MPa, respectively. That is, the stress rises with the increase in confining stress. However, the stress corresponding to 19 MPa is not significantly different from the stress corresponding to 15 MPa. The reason is as follows: Primary cracks inside the sample close under the action of confining stress, and the existence of confining stress increases the

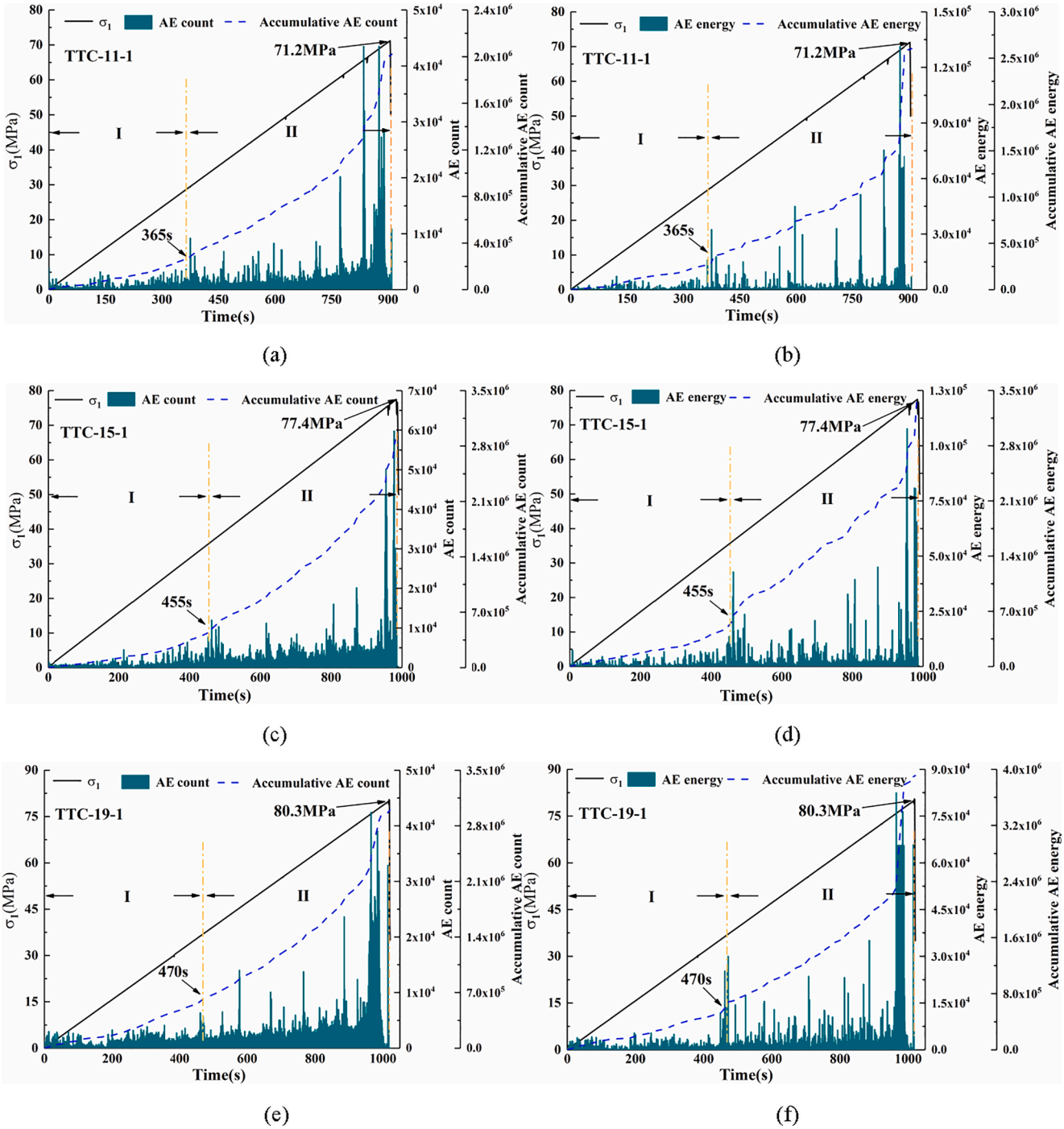

Fig. 5. Experimental results of AE under different confining stresses (a) AE count under 11 MPa; (b) AE energy under 11 MPa; (c) AE count under 15 MPa; (d) AE energy under 15 MPa; (e) AE count under 19 MPa; (f) AE energy under 19 MPa.

friction force that has to be overcome during friction sliding of cracks and hence inhibits crack development. When the confining stress is 19 MPa, the closure of primary cracks is accompanied by the generation of some secondary cracks under the action of high confining stress and gas pressure, which raises the damage degree of coal to some extent. As a result, local connection of cracks occurs earlier, and AE enters the accelerated growth stage earlier accordingly.

3.2. Determination of phase space dimension

According to the G-P algorithm, the value of phase space dimension m has a considerable influence on the correlation dimension D value of a specific time series. Therefore, it is necessary to select the appropriate phase space dimension before calculating the correlation dimension of AE time series. The variations of correlation dimension with phase space dimension under different gas pressures and confining stresses are displayed in Fig. 6 which reveals that the correlation dimension exhibits the same variation trend with the change of phase space dimension: The correlation dimension increases with the growth of phase space dimension, but it tends to stabilize and ceases increasing after the phase space dimension reaches a certain value. According to the previous study, AE time series exhibits good fractal characteristics when the correlation dimension becomes stable [35]. In this paper, the value of m at the moment when the correlation dimension starts to stabilize is taken

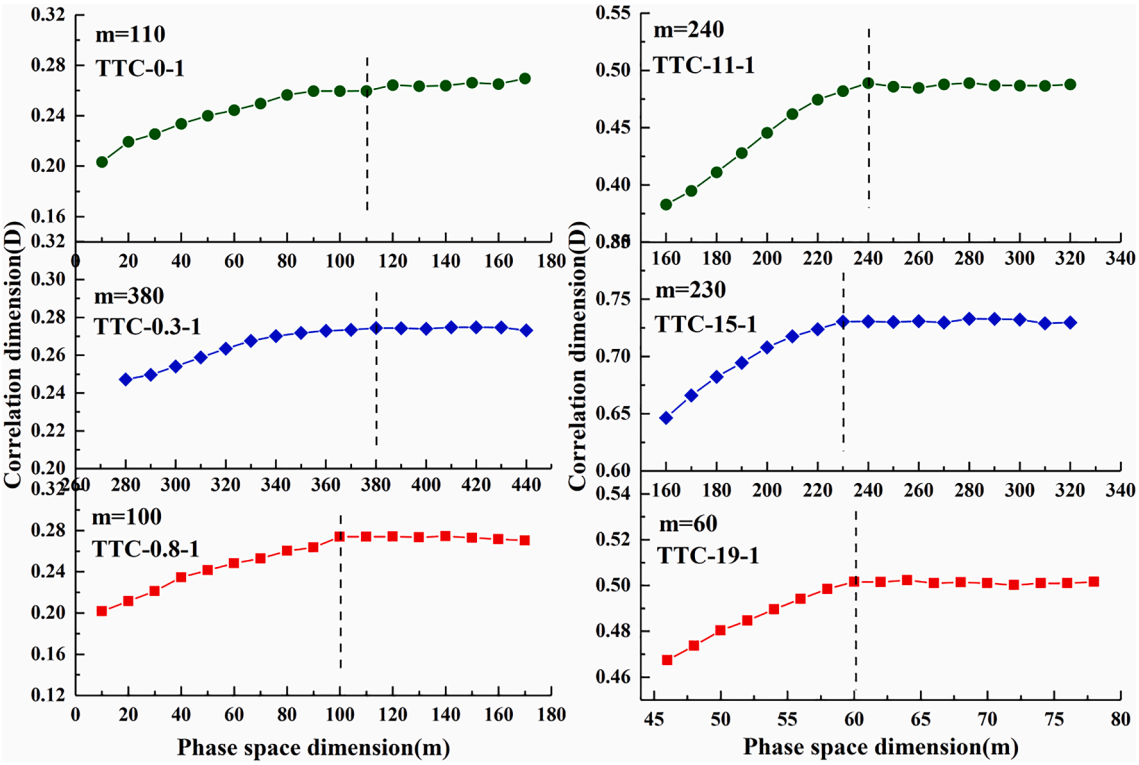

Fig. 6. Determination of phase space dimension (a) Under different gas pressures; (b) Under different confining stresses.

as the phase space dimension for subsequent calculations. From Fig. 6, the phase space dimensions under gas pressures 0 MPa, 0.3 MPa, and 0.8 MPa are taken as 110, 380, and 100, and those under confining stresses of 11 MPa, 15 MPa, and 19 MPa are taken as 240, 230, and 60, respectively.

3.3. Fractal characteristics of AE time series

AE time series under different gas pressures were calculated in accordance with the selected phase space dimensions. Furthermore, the relationship between lnr and $lnY(r)$ was obtained, and the points (lnr, $lnY(r)$) were subjected to linear fitting. According to the fitting results (Fig. 7), the correlation coefficients R^2 of fitted lines are all greater than 0.9, and lnr is strongly linearly correlated with $lnY(r)$, manifesting that the AE time series has obvious fractal characteristics in the whole fracturing process under different gas pressures. The correlation dimensions of AE time series under gas pressures of 0 MPa, 0.3 MPa and 0.8 MPa are 0.2596, 0.2716 and 0.2739, respectively. In short, a higher gas pressure means more obvious fractal characteristics of AE time series.

Fractals can describe the degrees of self-similarity [36–43], and the larger the correlation dimension, the stronger the degree of self-similarity of AE time series. When the gas pressure is 0 MPa and 0.3 MPa, the sample possesses strong resistance to deformation. Under the effect of stress, a large number of micro-cracks are generated and propagated, with sufficient friction sliding between the cracks. The entire damage and fracturing process is relatively complicated, and the sample undergoes discontinuous macroscopic fracturing. AE events in this process are also complicated; large and small AE signals appear alternately; and the appearance of large AE signals is paroxysmal. Thus, the self-similarity degree of AE time series is low under the two gas pressures. When the gas pressure is 0.8 MPa, the bearing capacity of the sample is weakened by gas which enters and fills the primary pores and cracks to further expand them and reduce the surface tension and friction between them. Under the action of stress, the sample gets severely damaged in an intense fracturing process, and the corresponding AE events mainly belong to large events. Thereby, the self-similarity degree of AE time series is the highest under this gas pressure.

The relationship between lnr and $lnY(r)$ under different confining stresses is illustrated in Fig. 8. The correlation coefficients R^2 of fitted lines are all greater than 0.9, and lnr and $lnY(r)$ share a good linear relationship. This result demonstrates that AE time series has evident fractal characteristics in the whole fracturing process under different confining stresses. The correlation dimensions of AE time series under confining stresses of 11 MPa, 15 MPa, and 19 MPa are 0.4889, 0.7238, and 0.5018, respectively. The correlation dimension grows first and then drops as the confining stress rises. The fractal characteristics of AE time series are the strongest under the confining stress of 15 MPa.

Under the confining stress of 11 MPa, the sample has weak resistance to deformation; the degree of closure of primary cracks is relatively low; cracks can connect locally under a smaller stress. Consequently, the sample experiences severe and intense failure and produces complex AE signal, so the self-similarity degree of AE time series is low. When the confining stress is 15 MPa, the degree of closure of primary cracks goes up; both the friction force that has to be overcome during friction sliding between cracks and the lateral supporting force that the confining stress gives to the coal increase, which decides that the instability and destruction of coal requires more energy. Resultantly, the destruction process is relatively smooth, and the self-similarity of AE time series is enhanced. When the confining stress is 19 MPa, under the action of high confining stress and gas pressure, primary cracks close and some secondary cracks occur, which raises the damage degree of coal, so that local connection of cracks occurs earlier. Due to the supporting effect by confining stress, the sample is of a higher crack extension and connection degree before instability and failure. Compared with the previous case (confining stress 15 MPa), the sample undergoes more severe fracturing and generates more active AE events under 19 MPa, and the

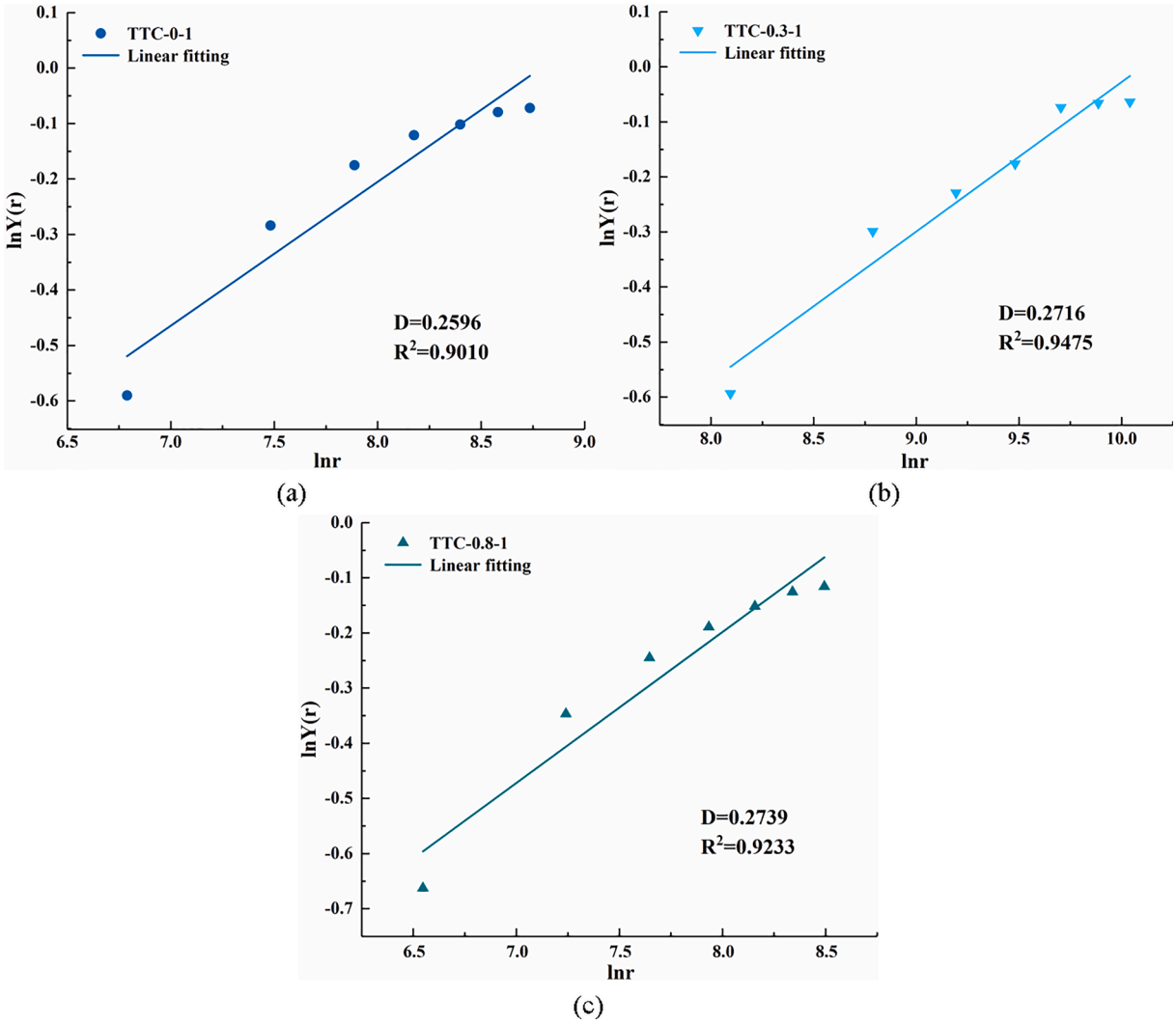

Fig. 7. Relationship between *lnr* and *lnY*(*r*) (a) Under the gas pressure of 0 MPa; (b) Under the gas pressure of 0.3 MPa; (c) Under the gas pressure of 0.8 MPa.

self-similarity degree of AE time series is lowered.

On the basis of the above analysis, it can be concluded that correlation dimension can reflect the damage degree of a loaded sample [29,30,34,35]. Hence, correlation dimension can be taken as a parameter to describe damage degree and mechanical properties of a coal sample.

The relationship between *lnr* and *lnY*(*r*) can reflect the overall fractal characteristics of AE time series. However, AE signals are dynamically varying process which occurs simultaneously with the damage and destruction of a coal sample. To obtain the variation law of fractal characteristics of AE in the whole damage and destruction process, the correlation dimensions of AE time series at different stress levels were calculated (Fig. 9).

It can be observed from Fig. 9 that the correlation dimension values differ significantly at different stress levels, but they vary in resembling trends under different gas pressures and different confining stresses. When the stress level is 0%-20%, the correlation dimension fluctuates. This is because coal contains primary pores and cracks with different numbers and sizes. At this time, the coal sample basically remains in the compaction stage where some primary pores and cracks close due to the continuous increase in stress while some cracks expand in a small range. The sample undergoes complicated damage evolution and produces extremely disordered AE events. When the stress level is 20%-55%, the correlation dimension shows an upward trend. This is because the coal sample has stepped into the elastic deformation stage. As the load increases, cracks begin to extend and connect locally. In this stage, the damage of the sample becomes localized, and the main fracture area gradually forms within the sample. With the damage and fracturing of the sample getting increasingly ordered and local, the AE events become more and more active and AE time series exhibit strong regularity. When the stress level exceeds 60%, the correlation dimension gradually decreases, reaching the minimum at the moment of sample failure. This is because the coal sample enters the yield deformation and failure stage. In this stage, stress is concentrated in the main fracture area; the sample begins to fail at an accelerate rate; and AE events increase significantly. When the stress level exceeds a certain value, elastic energy accumulated in the sample exceeds the energy storage threshold. Consequently, the main fracture area is completely penetrated, and macroscopic fractures occur in the sample. In this period, AE events are highly disordered, and the fractal characteristics of AE time series gradually weaken.

The correlation dimensions of AE time series under different conditions differ remarkably, but they share similar dynamic variation trends, indicating that the overall failure processes of samples under different true triaxial loading conditions are macroscopically consistent. The dynamic changes, i.e., fluctuation-increase-decrease, in correlation dimension can accurately reflect the damage evolution process of a sample. At the same time, the gradual reduction in the correlation dimension can be regarded as the precursor information for instability and damage of coal sample. This finding has guiding significance for preventing the occurrence of coal and rock gas dynamic disasters.

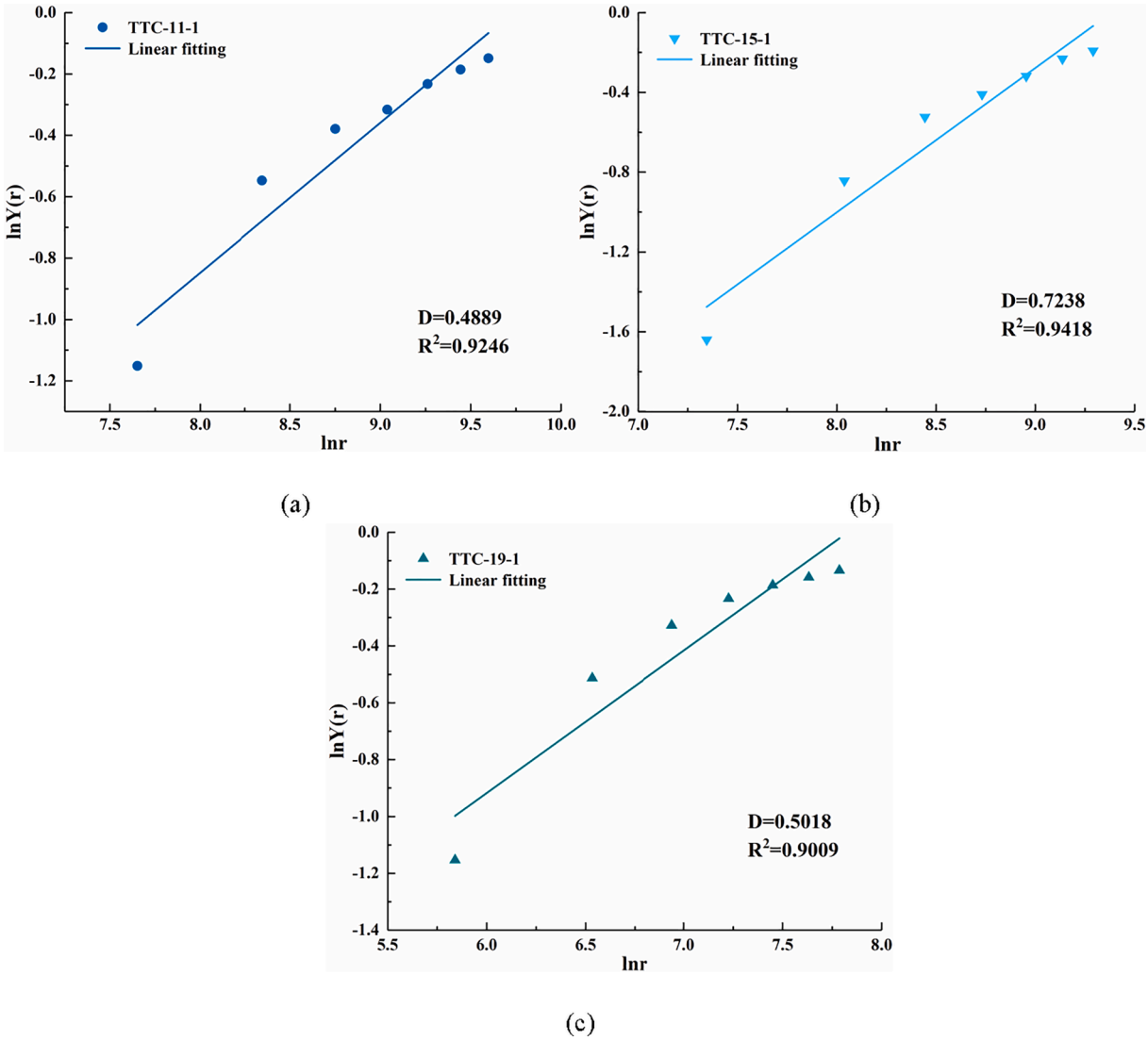

Fig. 8. Relationship between *lnr* and *lnY*(*r*) (a) Under the confining stress of 11 MPa; (b) Under the confining stress of 15 MPa; (c) Under the confining stress of 19 MPa.

4. Discussions

4.1. Effect of gas pressure on coal sample damage process

Gas can alter the mechanical properties of coal [15,16,17,44,45]. From Fig. 4, the strength of coal decreases with the rise of gas pressure. Gas, which exists in coal in two states (free gas or adsorbed gas), mainly exerts four stages (seepage, diffusion, adsorption, and desorption) of effects on the loading and fracturing process of coal.

Gas adsorbs on coal before the start of continuous loading. This process mainly involves free gas whose influence on the mechanical properties of a coal sample consists of two aspects: First, in the initial stage of adsorption, gas enters the sample and flows in primary pores and cracks in a free state. The continuously flowing high-pressure free gas further promotes the expansion and development of primary pores and cracks. Meanwhile, it expands the volume, reduces the density, and change the internal structure of the sample, eventually raising the damage degree. Second, after gas adsorption equilibrium is reached in the sample, free gas will adhere to the surface of adjacent cracks, which reduces the surface tension between micro-cracks. Macroscopically, the viscosity between micro-cracks is reduced; less friction force is needed to overcome friction sliding between the cracks; and less stress and energy is required for the extension and connection of micro-cracks. As a result, the coal sample whose strength drops loses stability and fails at an accelerated rate.

The increase in stress will result in elastic energy accumulation in coal. After the gas adsorption equilibrium is reached, adsorbed gas is stored in coal as gas potential energy. The failure process of a loaded coal sample is determined by the joint action of elastic energy and gas potential energy accumulated in the sample. With the continuous increase in load, micro-cracks develop and expand continuously. When cracks connect locally inside the sample, gas adsorbed inside the sample will be desorbed in a very short time and enter the locally connected fracture area, which accelerates the failure process of the sample. A higher gas pressure corresponds to greater gas potential energy stored in the sample, a larger amount of desorbed gas, and a stronger effect in accelerating sample failure.

A conclusion can be drawn that the decrease in the strength of gas-bearing coal is caused by the joint action of free gas and adsorbed gas whose mechanisms of action are different. Free gas mainly reduces the strength of the sample by altering its internal structure, while adsorbed gas reduces the strength by accelerating its failure process through gas desorption.

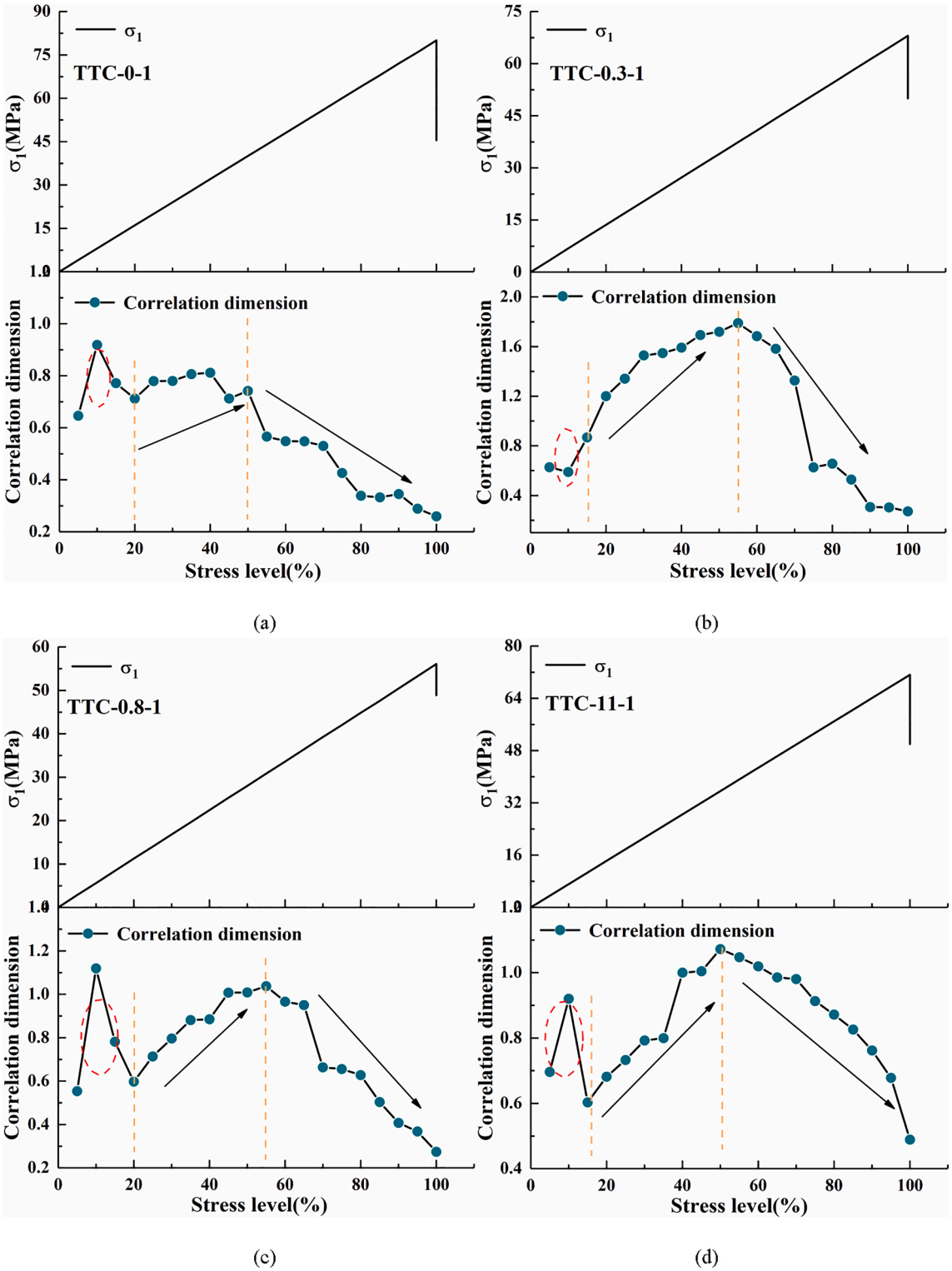

Fig. 9. Dynamic variations of correlation dimensions under different stress levels (a) Under the gas pressure of 0 MPa; (b) Under the gas pressure of 0.3 MPa; (c) Under the gas pressure of 0.8 MPa; (d) Under the confining stress of 11 MPa; (e) Under the confining stress of 15 MPa; (f) Under the confining stress of 19 MPa.

4.2. Effect of confining stress on coal sample damage process

In the true triaxial loading experiment, the change of confining stress will affect the expand of cracks in the coal sample, thereby further affecting its rupture process. With the increase of confining stress, the peak stress of the sample goes up continuously. The peak stress under the confining stresses of 15 MPa and 19 MPa are 8.7% and 12.8% higher than that under 11 MPa, respectively. This is because under the effect of confining stress, the original cracks closed in the coal sample. Meanwhile the existence of confining stress will increase the friction force that needs to be overcome during friction sliding between the cracks, thus inhibiting crack development. Moreover, confining stress provides

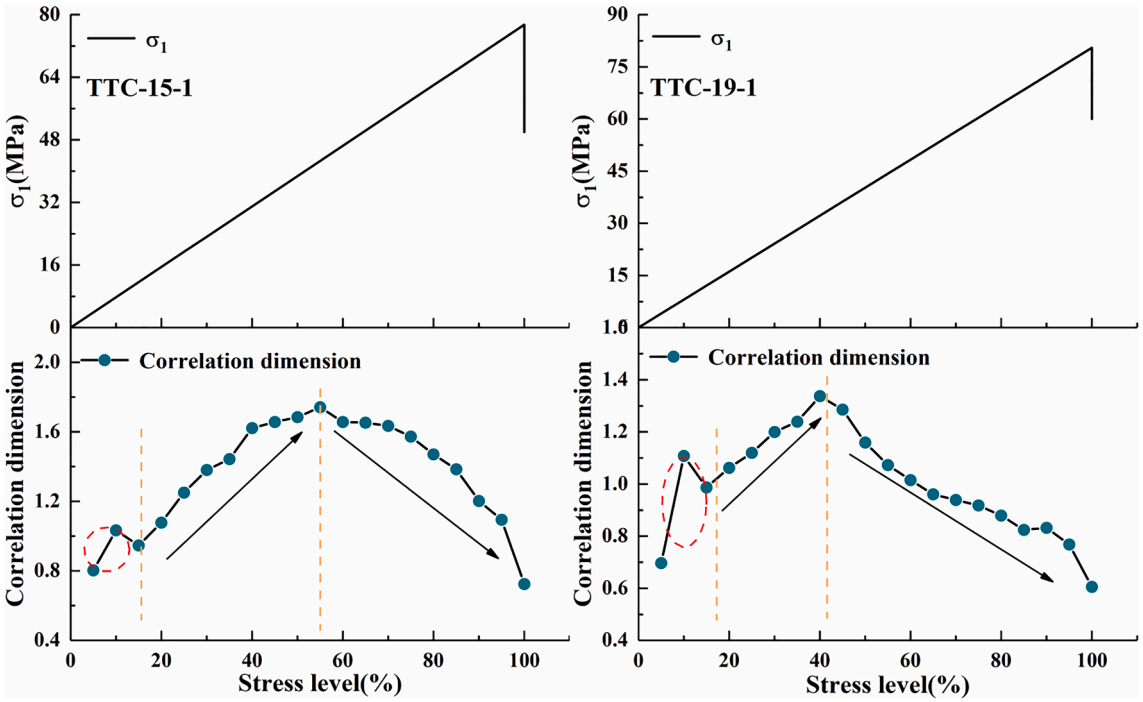

(e) (f)

Fig. 9. (*continued*).

lateral supporting force to coal sample, which improves the ability of coal sample to resist instability and damage. It demonstrates that confining stress enhances the strength, energy storage threshold, and bearing capacity of the sample. In addition, the strength of the sample under the confining stress of 15 MPa is 8.7% higher than that under 11 MPa, whereas the strength of the sample under 19 MPa is only 3.7% higher than that under 15 MPa. This suggests that confining stress does not always have positive effect on the mechanical properties of the sample. Under the action of high confining stress and gas pressure, primary cracks close while some secondary cracks occur, which raises the damage degree of coal to some extent, so that local connection of cracks occurs earlier. Excessive confining stress will accelerate the destruction of coal.

4.3. Effect of gas pressure on fractal characteristics

AE time series have fractal characteristics under different gas pressures. The correlation dimension gradually increases and the fractal characteristics are enhanced as the gas pressure rises. When the gas pressure is 0 MPa and 0.3 MPa, the sample owns strong bearing capacity. Under the action of stress, micro-cracks develop fully, and the entire damage and fracturing process is rather complicated. Correspondingly, AE events in this process are complicated, and the appearance of large AE signals is paroxysmal. Hence, the fractal characteristics of AE time series are weak under the two gas pressures. When the gas pressure is 0.8 MPa, the bearing capacity of the sample is greatly weakened under the joint action of free gas and adsorbed gas, and primary cracks further expand under the effect of free gas. Affected by stress, the sample gets severely damaged in an intense fracturing process with the desorption of a large amount of adsorbed gas. The corresponding AE events mostly belong to large events. Therefore, the fractal characteristics of AE time series are the most evident under this gas pressure.

4.4. Effect of confining stress on fractal characteristics

Under different confining stresses, AE time series have fractal characteristics which increase first and then decrease with the rise of confining stress. Fractal characteristics of AE time series are the strongest when the confining stress is 15 MPa. When the confining stress is low, the sample possesses weak ability to resist deformation and can experience local connection of cracks under a low stress. Therefore, the sample suffers relatively severe failure and generates complicate AE signals; the self-similarity degree of AE time series is low. After the confining stress is raised appropriately, the degree of closure of primary cracks increases; both the friction force required to overcome friction sliding between cracks and the lateral supporting force that the confining stress gives to the coal increase, which decides that the instability and destruction of coal requires more energy. Resultantly, the destruction process is relatively smooth, and the self-similarity of AE time series is enhanced. As the confining stress continues to increase, the sample is subjected to high confining stress and gas pressure, primary cracks close while some secondary cracks occur, which raises the damage degree of coal to some extent, so that local connection of cracks occurs earlier. Due to the supporting effect by confining stress, the sample is of a higher crack extension and connection degree before instability and failure; the sample undergoes more severe fracturing and generates more active AE events; and the self-similarity degree of AE time series is lowered.

5. Conclusions

(1) With the increasing of gas pressure, the peak stress of the sample decreases continuously. The peak stress under the gas pressures of 0.3 MPa and 0.8 MPa are 15% and 30% lower than that under 0 MPa, respectively, which suggests that the presence of gas weakens the bearing capacity and strength of the sample. With the increase of confining stress, the peak stress of the sample increases continuously. The peak stress under the confining

stresses of 15 MPa and 19 MPa are 8.7% and 12.8% higher than that under 11 MPa, respectively, which indicates that the confining stress promotes the strength, energy storage threshold, and bearing capacity of the sample.

(2) Based on accumulative AE count and accumulative AE energy, the process of AE variation can be divided into two stages, namely the slow growth stage and the accelerated growth stage. The duration of the slow growth stage shortens with the increase in gas pressure, while it lengthens with the increase in confining stress.

(3) AE time series display obvious fractal characteristics in the whole sample fracturing process under different gas pressures and different confining stresses. The correlation dimension can reflect the damage degree of a loaded coal sample and can thereby be regarded as a parameter to describe the damage degree and mechanical properties of a coal sample.

(4) The correlation dimension values differ significantly at different stress levels, but they share similar dynamic variation trends under different gas pressures and confining stresses. The dynamic changes, i.e., fluctuation-increase–decrease, in correlation dimension can accurately reflect the damage evolution process of a sample. In addition, the gradual reduction of the correlation dimension can be regarded as the precursor information for coal sample instability and damage. This finding has guiding significance for preventing the occurrence of coal and rock gas dynamic disasters.

CRediT authorship contribution statement

Ran Zhang: Methodology, Formal analysis, Data curation, Writing - original draft preparation. **Jie Liu:** Conceptualization, Methodology, Software, Supervision, Funding acquisition, Writing - review & editing. **Zhanyou Sa:** Supervision. **Zaiquan Wang:** Supervision. **Shouqing Lu:** Supervision, Funding acquisition. **Zhaoyang Lv:** Software.

Declaration of Competing Interest

The authors declare that they have no known competing financial interests or personal relationships that could have appeared to influence the work reported in this paper.

Acknowledgments

This work was supported by the National Natural Science Foundation of China (51504140; 51574153; 51804176; 51974169); Natural Science Foundation of Shandong Province (ZR2018PEE001); Key R&D Plan in Shandong Province (2018GSF120012); China Postdoctoral Science Foundation (2018M642632; 2019M652346); a Project of Shandong Province Higher Educational Science and Technology Program (J18KA187); Open Found of the Laboratory of Mining Disaster Prevention and Control (MDPC201903).

References

[1] Z.Y. Sa, J. Liu, J.Z. Li, Y.J. Zhang, Research on effect of gas pressure in the development process of gassy coal extrusion, Saf. Sci. 115 (2019) 28–35.
[2] J. Liu, R. Zhang, D.Z. Song, Z.Q. Wang, Experimental investigation on occurrence of gassy coal extrusion in coalmine, Saf. Sci. 113 (2019) 362–371.
[3] Q.Y. He, Y.C. Li, J.H. Xu, C.G. Zhang, Prediction of mechanical properties of igneous rocks under combined compression and shear loading through statistical analysis, Rock Mech. Rock Eng. 53 (2020) 841–859.
[4] X.J. Feng, Q.M. Zhang, The effect of backfilling materials on the deformation of coal and rock strata containing multiple goaf: a numerical study, Minerals 8 (6) (2018) 224.
[5] S.Q. Lu, C.F. Wang, Q.Q. Liu, Y.L. Zhang, J. Liu, Z.Y. Sa, L. Wang, Numerical assessment of the energy instability of gas outburst of deformed and normal coal combinations during mining, Process. Saf. Environ. Prot. 132 (2019) 351–366.
[6] Y.J. Liu, X.L. Li, Z.H. Li, P. Chen, T. Yang, Experimental study of the surface potential characteristics of coal containing gas under different loading modes (uniaxial, cyclic and graded), Eng. Geol. 249 (2019) 102–111.
[7] Z.J. Wen, E.R. Xing, S.S. Shi, Y.J. Jiang, Overlying strata structural modeling and support applicability analysis for large mining-height stopes, J. Loss Prevent. Proc. 57 (2018) 94–100.
[8] D.A. Lockner, J.D. Byerlee, V. Kuksenko, A. Ponomarev, A. Sidorin, Quasi-static fault growth and shear fracture energy in granite, Nature 350 (7) (1991) 39–42.
[9] S.J.D. Cox, P.G. Meredith, Microcrack formation and material softening in rock measured by monitoring acoustic emissions, Int. J. Rock Mech. Min. Sci. Geomech. Abstr. 30 (1993) 11–24.
[10] M.C. He, J.L. Miao, J.L. Feng, Rock burst process of limestone and its acoustic emission characteristics under true-triaxial unloading conditions, Int. J. Rock Mech. Min. Sci. 47 (2) (2010) 286–298.
[11] S.M. Liu, X.L. Li, D.K. Wang, M.Y. Wu, G.Z. Yin, M.H. Li, Mechanical and acoustic emission characteristics of coal at temperature impact, Nat. Resour. Res. 29 (3) (2019) 1755–1772.
[12] X. Wang, Z.J. Wen, Y.J. Jiang, H. Huang, Experimental study on mechanical and acoustic emission characteristics of rock-like material under non-uniformly distributed loads, Rock Mech. Rock Eng. 51 (2018) 729–745.
[13] Z.J. Wen, X. Wang, L.J. Chen, G. Lin, H.L. Zhang, Size effect on acoustic emission characteristics of coal-rock damage evolution, Adv. Mater Sci. Eng. 2017 (2017) 3472485.
[14] S.M. Liu, X.L. Li, Z.H. Li, P. Chen, X.L. Yang, Y.J. Liu, Energy distribution and fractal characterization of acoustic emission (AE) during coal deformation and fracturing, Measurement 136 (2019) 122–131.
[15] S.Q. Lu, Y.L. Zhang, Z.Y. Sa, S.F. Si, Evaluation of the effect of adsorbed gas and free gas on mechanical properties of coal, Environ. Earth. Sci. 78 (2019) ID218.
[16] Y. Niu, C.J. Wang, E.Y. Wang, Z.H. Li, Experimental study on the damage evolution of gas-bearing coal and its electric potential response, Rock. Mech. Rock. Eng. https://doi.org/10.1007/s00603-019-01839-z.
[17] M.Y. Wei, J.S. Liu, D. Elsworth, S.J. Li, F.B. Zhou, Influence of gas adsorption induced non-uniform deformation on the evolution of coal permeability, Int. J. Rock Mech. Min. Sci. 114 (2019) 71–78.
[18] S.Q. Lu, Y.L. Zhang, Z.Y. Sa, S.F. Si, L.Y. Shu, L. Wang, Damage-induced permeability model of coal and its application to gas predrainage in combination of soft coal and hard coal, Energy. Sci. Eng. 7 (4) (2019) 1352–1367.
[19] Y.K. Ma, E.Y. Wang, Z.H. Li, J. Liu, Z.S. Du, Methane sorption and seepage in coal and characteristics of acoustic emission, Chin. J. Rock Mech. Eng. 37 (4) (2012) 641–646.
[20] H.B. Zhao, G.Z. Yin, H.H. Li, Z.W. Wang, Analysis on AE characteristic and its confining pressure effect of outburst coal containing gas, J. Chongqing. Univ. 36 (11) (2013) 101–107.
[21] G.Z. Yin, H. Qin, G. Huang, Experimental study of characteristics of seepage and acoustic emission of gas-filled coal under different stress paths, Chin. J. Rock Mech. Eng. 32 (7) (2013) 1315–1320.
[22] Y. Niu, Z.H. Li, H.H. Wang, J.L. Wang, S.J. Liu, S. Yin, Y.H. Kong, S. Hong, Experimental study on characteristics of acoustic emission for coal containing gas damaged evolution under loading, Indus. Mine. Auto. 42 (6) (2016) 37–41.
[23] X.G. Kong, E.Y. Wang, S.B. Hu, Z.H. Li, X.F. Liu, B.F. Fang, T.Q. Zhan, Critical slowing down on acoustic emission characteristics of coal containing methane, J. Nat. Gas Sci. Eng. 24 (2015) 156–165.
[24] B.B. Mandelbrot, Fractals: Forms, Chance and Dimension, W. H. Freeman & Co Ltd., San Francisco, 1977.
[25] H.P. Xie, J.A. Wang, M.A. Kwaśniewski, Multi-fractal characterization of rock fracture surfaces, Int. J. Rock Mech. Min. Sci. 36 (1) (1999) 19–27.
[26] X.G. Yin, S.L. Li, H.Y. Tang, Study on strength fractal features of acoustic emission in process of rock failure, Chin. J. Rock Mech. Eng. 19 (2005) 114–118.
[27] H.P. Xie, J.F. Liu, Y. Ju, G. Li, L.Z. Xie, Fractal property of spatial distribution of acoustic emissions during the failure process of bedded rock salt, Int. J. Rock Mech. Min. Sci. 48 (2011) 1344–1351.
[28] X.Z. Wu, X.X. Liu, Z.Z. Liang, X. You, M. Yu, Experimental study of fractal dimension of AE serials of different rocks under uniaxial compression, Rock. Soil. Mech. 33 (12) (2012) 3561–3569.
[29] X.G. Kong, E.Y. Wang, S.B. Hu, R.X. Shen, X.L. Li, T.Q. Zhan, Fractal characteristics and acoustic emission of coal containing methane in triaxial compression failure, J. Appl. Geophys. 124 (2016) 139–147.
[30] D.X. Li, E.Y. Wang, X.G. Kong, X.R. Wang, C. Zhang, H.S. Jia, H. Wang, J.F. Qian, Fractal characteristics of acoustic emissions from coal under multi-stage true-triaxial compression, J. Geophys. Eng. 15 (2018) 2021–2032.
[31] Z.B. Zhang, E.Y. Wang, N. Li, Fractal characteristics of acoustic emission events based on single-link cluster method during uniaxial loading of rock, Chaos. Soliton. Fract. 104 (2017) 298–306.
[32] P. Grassberger, On the fractal dimension of the Henon attractor, Phys. Lett. A 97 (1983) 224–229.
[33] P. Grassberger, I. Procaccia, Dimensions and entropies of strange attractors from a fluctuating dynamics approach, Physica D 13 (1984) 34–54.
[34] D.X. Li, E.Y. Wang, X.G. Kong, Ali Muhammad, D.M. Wang, Mechanical behaviors and acoustic emission fractal characteristics of coal specimens with a pre-existing flaw of various inclinations under uniaxial compression, Int. J. Rock Mech. Min. Sci. 116 (2019) 38–51.
[35] D.X. Li, E.Y. Wang, X.G. Kong, H.S. Jia, D.M. Wang, Ali Muhammad, Damage precursor of construction rocks under uniaxial cyclic loading tests analyzed by acoustic emission, Constr. Build. Mater. 206 (2019) 169–178.
[36] J. Liu, E.Y. Wang, Z.H. Li, Y.K. Ma, Multi-fractal characteristics of surface potential of coal during the fracture, J. Chin Coal Soc. 38 (09) (2013) 1616–11020.

[37] S.B. Hu, E.Y. Wang, Z.H. Li, R.X. Shen, J. Liu, Time-varying multifractal characteristics and formation mechanism of loaded coal electromagnetic radiation, Rock Mech. Rock Eng. 47 (5) (2014) 1821–1838.
[38] B. Kong, E.Y. Wang, Z.H. Li, X.R. Wang, L. Chen, X.G. Kong, Nonlinear characteristics of acoustic emissions during the deformation and fracture of sandstone subjected to thermal treatment, Int. J. Rock Mech. Min. Sci. 90 (2016) 43–52.
[39] X.G. Kong, E.Y. Wang, X.Q. He, D.X. Li, Q.L. Liu, Time-varying multifractal of acoustic emission about coal samples subjected to uniaxial compression, Chaos. Soliton. Fract. 103 (2017) 571–577.
[40] X.L. Li, Z.H. Li, E.Y. Wang, Y.P. Liang, B.L. Li, P. Chen, Y.J. Liu, Pattern recognition of mine microseismic and blasting events based on wave fractal features, Fractals 26 (03) (2018) 1850029.
[41] L.M. Qiu, D.Z. Song, X.Q. He, E.Y. Wang, Z.L. Li, S. Yin, M.H. Wei, Y. Liu, Multifractal of electromagnetic waveform and spectrum about coal rock samples subjected to uniaxial compression, Fractals 28 (04) (2020) 2050061.
[42] J.J. Feng, E.Y. Wang, Q.S. Huang, H.C. Ding, Y.K. Ma, Study on coal fractography under dynamic impact loading based on multifractal method, Fractals 28 (01) (2020) 2050006.
[43] R. Zhang, J. Liu, Z.Y. Sa, Z.Q. Wang, S.Q. Lu, C.F. Wang, Experimental investigation on multi-fractal characteristics of acoustic emission of coal samples subjected to true triaxial loading-unloading, Fractals https://doi.org/10.1142/S0218348X20500929.
[44] G.X. Xie, Z.Q. Yin, L. Wang, Z.X. Hu, C.Q. Zhu, Effects of gas pressure on the failure characteristics of coal, Rock Mech. Rock Eng. 50 (2017) 1711–1723.
[45] S.G. Wang, D. Elsworth, J.S. Liu, Mechanical behavior of methane infiltrated coal: the roles of gas desorption, stress level and loading rate, Rock Mech. Rock Eng. 46 (2013) 945–958.